Journal of Chemical Health Risks

www.jchr.org

JCHR (2024) 14(2), 2718-2724 | ISSN:2251-6727

Antineoplastic and Antioxidant Activity of Engineered Andrographolide Selenium Nanoparticles

[1]Archana*, [2]Rohit Deshmukh

[1*]Research Scholar, Institute of pharmaceutical research, GLA University, Mathura-281406

[2]Associate Professor, Institute of pharmaceutical research, GLA University, Mathura-281406

(Received: 07 January 2024 Revised: 12 February 2024 Accepted: 06 March 2024)

KEYWORDS

Nanotechnology

Selenium

Cancer

Andrographolide

spectroscopy

ABSTRACT:

Introduction: Nanotechnology refers to any technological advancement that operates on the nanoscale and has diverse practical applications. Nanotechnology encompasses the creation and use of physical, chemical, and biological processes at scales that range from atoms to submicron dimensions.

Objectives: The objective of this research is to synthesize nanoparticles of selenium employing Andrographolide via an eco-friendly approach.

Methods: The green nanoparticles were analyzed by ultraviolet-visible spectroscopy, FT-IR, and TEM.

Results: The dimensions of the synthesized selenium nanoparticles (SeNPs) in Andrographolide were determined to vary between 12 and 160 nanometers, based on the analysis of transmission electron microscopy (TEM) images. The selenium nanoparticles exhibited antioxidant activity ranging from 66.7% to 83.7% in terms of their ability to block free radicals.

Conclusions: Higher nanoparticle concentration results in reduced cancerous cell viability. The presence of produced nanoparticles of selenium clearly demonstrates their ability to inhibit cancer growth, with the extent of this action depending on the dosage.

1. Introduction

Nanotechnology is a field that focuses on the manipulation of materials at the nanoscale scale, which is one billion times smaller than a meter [1]. Nanotechnology refers to any technological advancement that operates on the nanoscale and has diverse practical applications. Nanotechnology encompasses the creation and use of physical, chemical, and biological processes at scales that range from atoms to submicron dimensions. Additionally, it involves the integration of these resulting nanomaterials into larger systems [2, 3]. Selenium (Se) is an essential trace element found in human bodies. Selenium is present in proteins in the form of selenocysteine (Sec), which is commonly known as selenoproteins. The significance of selenium in human nutrition is attributed to its presence in enzymes, which play a crucial role in protecting the organism from the harmful effects of oxidative stress [4, 5]. Oxidoreductase in selenoproteins plays a crucial role in maintaining the balance of redox reactions in the body. Due to the little toxicity of selenium nanoparticles (SeNPs), they have been extensively studied for their potential in treating various oxidative stress and inflammatory conditions. Thus, SeNPs provide a means to deliver diverse drugs to the specific location of action [6]. The present study demonstrates the production of selenium nanoparticles (SeNPs) employing Andrographolide.

The utilization of medicinal plant extracts to produce nanoparticles through environmentally friendly methods has lately become widely recognized. Phytochemicals, namely, form the fundamental structure of plants and have the ability to easily generate nanoparticles that have reduced toxicity. With the increasing awareness of the advantages of Andrographolide, researchers have started to show interest in them [7].

Journal of Chemical Health Risks

www.jchr.org

JCHR (2024) 14(2), 2718-2724 | ISSN:2251-6727

Andrographolide is a labdane diterpenoid compound that has been extracted from the stem and leaves of the Andrographis paniculata plant. Andrographolide has been investigated for its impact on cellular signaling, immunomodulation, and stroke.[2] Research has demonstrated that andrographolide has the ability to attach itself to a range of protein targets, such as NF-κB and actin, through covalent modification. [8]

2. Objectives

The objective of this research was to synthesize nanoparticles of selenium employing Andrographolide via an eco-friendly approach.

3. Methods

Production of a broth containing andrographolide

Andrographolide, at a concentration of 180 mg, was dispersed in sixty milliliters of deionized water and agitated at room temperature for a duration of 1 hour. Subsequently, the andrographolide solution underwent filtration using Whatman paper number 1. The filtrate was taken out and subjected to a second filtration using a micro filter to produce the andrographolide broth.

Synthesis of selenium nanoparticles stabilized with andrographolide

A solution was prepared by dissolving 3 mL of Andrographolide broth in 24 mL of deionized water. Subsequently, 3 mL of a solution containing 20 millimolar concentration of selenium salt was introduced and vigorously mixed at ambient temperature for a duration of 3 hours. The solution's color transitioned from yellow to reddish brown when the andrographolide stabilized-SeNPs were formed.

Characterization of andrographolide-stabilized silver nanoparticles

The evaluation of selenium nanoparticles stabilized by andrographolide was conducted using UV-visible spectrophotometric examination, transmission electron microscopy (TEM), Fourier transform infrared (FTIR) spectroscopy, and X-ray diffractometry (XRD). The absorption spectra of colloidal solutions containing andro-SeNPs were measured across a wavelength range of 200–800 nm. Andro-SeNPs colloidal solutions were applied onto carbon film-supported copper grids for TEM experiments and examined using a TEM instrument from FEI Company in Oregon, USA. The FTIR spectra were obtained using an Attenuated Total Reflectance (ATR) FTIR spectrophotometer, namely the Bruker TENSOR 27 model from the Netherlands. The measurements were conducted in the solid state using a standard Pike ATR cell, covering a range of 4000–600 cm–1. The dried powder of andro-SeNPs underwent additional analysis using X-ray diffraction. The X-ray diffraction was performed using a PANalytical Empyrean powder diffractometer, with an X-ray source emitting CuKα radiation ($\lambda = 0.15418$ Å). The investigation was conducted using a traditional 2theta scan spanning from 20 to 80 degrees.

Cytotoxicity assays

The cytotoxicity of SeNPs was assessed using the 3-(4,5-dimethylthiazolyl-2)-2,5 diphenyltetrazolium bromide (MTT) assay, which measures the rate of cell proliferation and detects a decrease in cell viability resulting from apoptosis or necrosis caused by metabolic processes. The yellow chemical MTT is converted into an insoluble purple formazan by mitochondrial dehydrogenases within live cells. To dissolve the formazan crystal, a solvent such as dimethyl sulfoxide is used. The concentration of formazan is subsequently measured using absorption spectroscopy within the wavelength range of 500–600 nm. The MCF-7 cell lines were used as models for malignant mammalian cell lines, respectively. The cells were arranged in a 96-well plate. After a duration of 24 hours, a concentration of 100 micrograms per milliliter of andro-SeNPs was introduced to the plate. The control group consisted of cells that were not exposed to any treatment chemicals. The cells were cultured and analyzed at 24, 48, and 72 hours to assess their vitality. Following the treatment, 10 microliters of a 5 microgram per milliliter MTT stock solution was introduced into each well and allowed to incubate for 4 hours at a temperature of 37 degrees Celsius. The medium was extracted, and 150 µL of dimethyl sulfoxide (DMSO) was introduced into each well to facilitate the dissolution of the formazan crystals. The measurement of the solution was conducted at a wavelength of 570 nm using a Varioskan™ LUX multimode microplate reader manufactured by Thermo Scientific in the United States. The experiments were

Journal of Chemical Health Risks
www.jchr.org
JCHR (2024) 14(2), 2718-2724 | ISSN:2251-6727

conducted three times. Cell viability was determined by applying the following mathematical formula:

$$\text{Cell viability \%} = \text{Absorbance of treated cell} / \text{Absorbance of control cell} * 100$$

Antioxidant activity

The DPPH assay for evaluating the ability of Andrographolide induced SeNPs to scavenge free radicals was conducted following the procedure described in the study by Rajeshkumar et al. [9]. The amounts of Andrographolide synthesized selenium nanoparticles (5, 10, 15, 20, and 25 µg/mL) were added to 1 mL of DPPH. Then, 450 µl of TrisHCl buffer was added, and the mixture was incubated for 30 minutes. The assessment of free radical scavenging was conducted using the quantification of absorbance at a wavelength of 517 nm. BHT was employed as a control. Ascorbic acid was used as a standard chemical. The inhibition % was calculated using the following equation.

$$\%\text{inhibition} = \frac{\text{absorbance of control} - \text{absorbance of sample}}{\text{absorbance of control}} \text{x100}$$

4. Results

UV-Vis Analysis

By employing UV-visible spectroscopy, it was initially confirmed that SeNPs were created when andrographolide extract was used (Figure 1). The readings were taken at certain intervals, including 6, 12, 24, 48, and 72 hours. In its UV spectra, SeNPs showed an absorption peak at 390 nm.

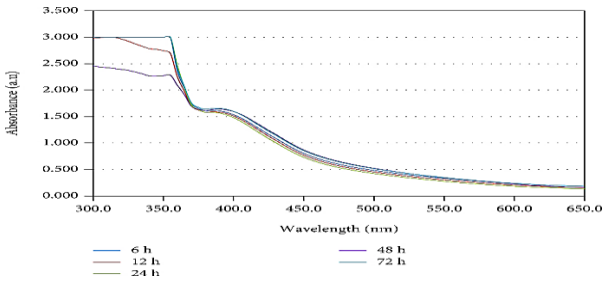

Figure 1: Analysis of selenium nanoparticles using UV-Visible spectroscopy.

FTIR Analysis

The many functional groups involved in the reduction process can be seen by selenium nanoparticles' Fourier transform infrared spectroscopy (Figure 1). Two prominent peaks in the selenium n NPs' Fourier transform infrared spectra can be found at 3423 cm-1 and 1653 cm-1, respectively, which are connected to the tensions of the hydroxyl groups. The functional groups of C = O, NH, and NH2 are represented by the peak that was found in the 1290 cm1 range. These functional groups are what give selenium NPs their stability. By converting sodium selenite to elemental selenium, these functional groups are also referred to as reducing agents [22].

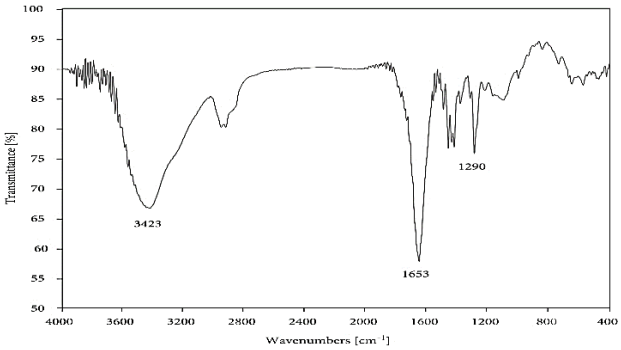

Figure 2: Fourier transform infrared spectroscopy (FTIR) spectra of selenium nanoparticles.

XRD Analysis

Figure 3 displays the XRD spectrum created from selenium nanoparticles. The well-crystallized selenium NPs may have formed as a result of the sharp and narrow peaks. Peaks relating to the crystal planes of (100), (101), (110), (102), (111), (201), (112), and (202) of the standard were centered at 23.5°, 29.2°, 41.4°, 43.3°, 52.5°, 55.7°, and 62.7°. Additionally, the produced spectrum shows that the synthesized selenium NPs are polymorphic [21].

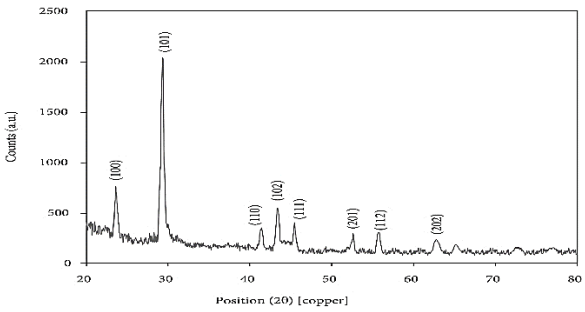

Figure 3:X-ray diffraction (XRD) patterns of selenium nanoparticles.

Journal of Chemical Health Risks

www.jchr.org

JCHR (2024) 14(2), 2718-2724 | ISSN:2251-6727

SEM ANALYSIS

Scanning electron microscopy images of selenium NPs confirmed the formation of these nanoparticles. From the image shown in Figure it can be seen that many of the nanoparticles formed are spherical.

EDX ANALAYSIS

The EDX spectrum was used to identify the selenium as nanoscale particles derived from andrographaloid. Figure 4 shows the EDX spectrum created from the synthesized selenium NPs. Along with oxygen and selenium, silicon and carbon elements were also seen in the spectrum of selenium oxide NPs, indicating the existence of some contaminants from the biological creation of nanoparticles.

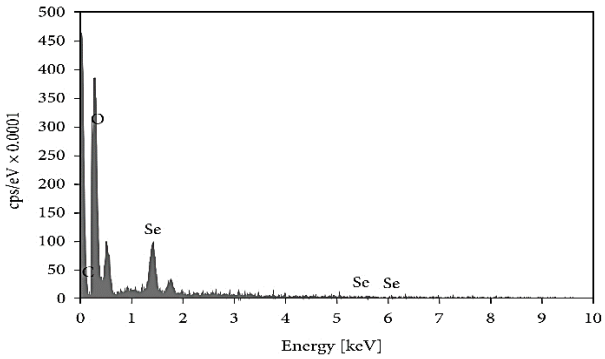

Figure 4: Energy dispersive X-ray (EDX) spectrums of selenium nanoparticles.

TEM Analysis

The TEM picture obtained of synthetic selenium NPs is displayed in Figure 5. The image demonstrated the spherical shape and size of the synthesized NPs, which are ideal for use in a variety of sectors. The dispersion of synthesized NPs was primarily in the range of 100 nm, according to TEM evaluation of particle size. Smaller nanoparticles can more easily enter cells, where they can disrupt diseases' functions and ultimately kill them.

Thermal analysis

Figure 6 illustrates the results of a thermal examination of the synthesized selenium NPs using TGA analysis. The removal of volatiles and moisture from the surface of the nanoparticles may be what caused the initial stage of weight loss of selenium NPs to be seen in the range of 100°C. The widespread breakdown of selenium NPs in the second stage, which was between 100 and 480°C, resulted in a noticeable weight loss. In addition, selenium nanoparticles showed signs of heat deterioration up to 800°C [17].

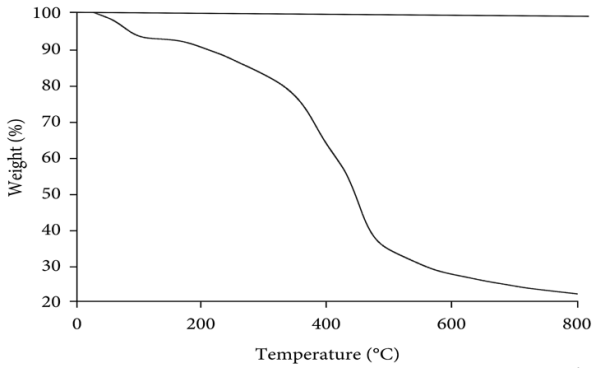

Figure 6: Investigation of selenium nanoparticles using thermogravimetry

Cytotoxicity

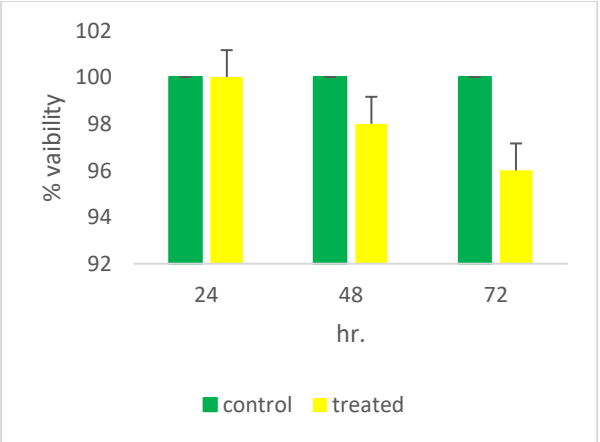

Figure 7: MTT assay evaluation of andro-SeNPs' cytotoxicity towards carcinogenic (MCF-7) mammalian cell lines. Andro-SeNPs were incubated with MFC-7 for 24, 48, and 72 hours at a concentration of 100 g/mL. The same cells' 100% vitality was checked using the same cells devoid of andro-SeNPs as a control. The results are the mean value plus standard deviation (error bar) from two separate tests that were performed in triplicate (n = 6).

Antioxidant activity

By lessening the cellular oxidative damage brought on by free radicals, antioxidants function as a defense mechanism to stop the body from developing serious

Journal of Chemical Health Risks
www.jchr.org
JCHR (2024) 14(2), 2718-2724 | ISSN:2251-6727

chronic diseases [10]. By using the DPPH method, the antioxidant activity of selenium nanoparticles mediated by andrographaloid was examined. The selenium nanoparticles demonstrated considerable free radical inhibition higher at 50 L concentration in a dose-dependent manner, as shown in Figure 8. The selenium nanoparticles displayed free radical inhibition of 66.7% at 10 µL concentration and 83.7% at 50 µL concentration.

Figure 8: Free radical scavenging activity of Andrographolide extract mediated SeNPs.

5. Discussion

Andro-SeNPs were produced by reducing selenium salt in a solution containing andrographolide. Figure 1 displays the spectrum of absorption of the resulting andro-SeNPs. The brown colour of the solution is a result of the distinct absorption as well as scattering of localised surface plasmon resonances (SPR) that reach their peak at 390 nm [23]. Fourier transform infrared (FTIR) spectroscopy reveals that the purified andrographolide and the A. andrographolide capsules have the same functional groups as those found on the surface of the as-synthesized andro-SeNPs. The X-ray diffraction (XRD) analysis indicates that the andro-SeNPs exhibit a high level of crystallinity, with a face centred cubic (fcc) metallic silver structure. The average size of the crystallites is estimated to be 100 nm using the Scherrer equation. The transmission electron microscopy (TEM) technique was used to examine the size and morphology of the andro-SeNPs. The analysis showed the presence of both spherical and irregularly shaped nanoparticles. The increased NP diameter observed using Dynamic Light Scattering (DLS) could be attributed to the aggregation of andro-SeNPs in the solution. Additionally, it may also be influenced by the presence of the stabilizing andrographolide layer and the hydration sphere, which cannot be evaluated using Transmission Electron Microscopy (TEM).

Trigonal selenium nanorods were formed through the microbial synthesis of SeNPs using the non-pathogenic bacterium Zooglea ramigera [11]. Previous studies conducted FT-IR analysis on selenium nanoparticles synthesized using broccoli. The analysis showed distinct peaks at 3235, 1595, 1407, and 1099 cm-1, which corresponded to the existence of aliphatic ether's O-H stretch, N-H bend, C-F stretch, and C-O stretch, respectively. SeNPs (at a concentration of 64 g/mL) have the potential to replace antibiotics for the treatment of bacterially induced skin diseases. This is because they effectively stopped the growth of Streptococcus agalactiae, Escherichia fergusonii, and Pseudomonas aeruginosa [12]. SeNPs produced utilizing Clausea dentata showed high larvicidal action and enhanced concentration against Culex quinquefasciatus, Aedes aegypti, and Anopheles stephensi fourth instar larvae [13]. Researchers found that SeNPs induced apoptosis, leading to the death of MCF-7 cells. Additionally, the combination of SeNPs with doxorubicin demonstrated remarkable anti-cancer properties [14]. The researchers in the study conducted by Mojtaba Shakibaie et al. (2015) utilized Bacillus species for the microbial production of SeNPs to combat Candida albicans and Aspergillus fumigatus. The findings demonstrated significant antifungal activity, indicating potential effectiveness. Azoarcus sp. was employed to biosynthesize SeNPS by converting selenite to Se and generating spherical SeNPs. Selenium nanoparticles coated with lignin were produced using dehydrated Vitis vinifera (raisin) extract [15]. The researchers utilized the flower extract of Bougainvillaea spectabilis to create selenium nanoparticles (SeNPs) by a biogenic process. The produced SeNPs were stable and hollow, with an average size of 24.24 ± 2.95 nm [16]. The cytotoxic impact of SeNPs and X-rays on lung cancer cell lines was validated through treatment. Lung cancer cells undergo programmed cell death, known as apoptosis, which is supported by the participation of Selenium Nanoparticles

Journal of Chemical Health Risks

www.jchr.org

JCHR (2024) 14(2), 2718-2724 | ISSN:2251-6727

(SeNPs) in the activation of caspase-3 and its subsequent target [17–22].

6. Conclusion

The findings demonstrated that selenium nanoparticles, which were produced using the biological synthesis method utilizing andrographolide, exhibited favorable physical characteristics when tested against cancer cell types. The synthesized nanoparticles were confirmed to have favorable structural characteristics using several analysis methods. Furthermore, based on the findings, it was anticipated that the synthesized nanoparticles effectively inhibit the proliferation of cancer cells under ideal conditions. Selenium nanoparticles possess favorable anticancer qualities and can effectively battle cancer ailments.

Refrences

1. S. Ramya, T. Shanmugasundaram, and R. Balagurunathan, “Biomedical potential of actinobacterially synthesized selenium nanoparticles with special reference to anti-biofilm, anti-oxidant, wound healing, cytotoxic and anti-viral activities,” Journal of Trace Elements in Medicine & Biology, vol. 32, pp. 30–39, 2015.
2. R. R. Mishra, S. Prajapati, J. Das, T. K. Dangar, N. Das, and H. Thatoi, “Reduction of selenite to red elemental selenium by moderately halotolerant Bacillus megaterium strains isolated from Bhitarkanika mangrove soil and characterization of reduced product,” Chemosphere, vol. 84, no. 9, pp. 1231–1237, 2011.
3. A. H. Shar, M. N. Lakhan, J. Wang et al., “Facile synthesis and characterization of selenium nanoparticles by the hydrothermal approach,” Digest Journal of Nanomaterials and Biostructures, vol. 14, no. 4, pp. 867–872, 2019.
4. S. Kanchi, Inamuddin, and A. Khan, “Biogenic synthesis of selenium nanoparticles with edible mushroom extract: evaluation of cytotoxicity on prostate cancer cell lines and their antioxidant, and antibacterial activity,” Biointerface Research in Applied Chemistry, vol. 10, no. 6, pp. 6629–6639, 2020.
5. N. Filipović, D. Ušjak, M. T. Milenković et al., “Comparative study of the antimicrobial activity of selenium nanoparticles with different surface chemistry and structure,” Frontiers in Bioengineering and Biotechnology, vol. 8, p. 1591, 2021.
6. M. Z. A. M Jaffar and A. N Zailan, “Antimicrobial resistance (amr)-forecast for 30 countries in Europe,” Science Heritage Journal, vol. 5, no. 2, pp. 44–48, 2021.
7. W.-F. Lai, “Development of hydrogels with self-healing properties for delivery of bioactive agents,” Molecular Pharmaceutics, vol. 18, no. 5, pp. 1833–1841, 2021.
8. Z. Wang, H. Xiang, P. Dong et al., “Pegylated azelaic acid: synthesis, tyrosinase inhibitory activity, antibacterial activity and cytotoxic studies,” Journal of Molecular Structure, vol. 1224, p. 129234, 2021.
9. H. Moradpoor, M. Safaei, F. Rezaei et al., “Optimisation of cobalt oxide nanoparticles synthesis as bactericidal agents,” Open Access Macedonian Journal of Medical Sciences, vol. 7, no. 17, pp. 2757–2762, 2019.
10. J. E. Frencken, P. Sharma, L. Stenhouse, D. Green, D. Laverty, and T. Dietrich, “Global epidemiology of dental caries and severe periodontitis - a comprehensive review,” Journal of Clinical Periodontology, vol. 44, no. 18, pp. S94–S105, 2017.
11. H. Moradpoor, M. Safaei, H. R. Mozaffari et al., “An overview of recent progress in dental applications of zinc oxide nanoparticles,” RSC Advances, vol. 11, no. 34, pp. 21189–21206, 2021.
12. J. C. Farges, B. Alliot-Licht, E. Renard et al., Dental Pulp Defence and Repair Mechanisms in Dental Caries, Mediators of Inflammation, Article ID 230251, 2015.
13. F. Cura, A. Palmieri, A. Girardi, M. Martinelli, L. Scapoli, and F. Carinci, “Lab-Test® 4: Dental caries and bacteriological analysis,” Dental Research Journal, vol. 9, no. 2, pp. 139–141, 2012.
14. M. Taran, M. Safaei, N. Karimi, and A. Almasi, “Benefits and application of nanotechnology in environmental science: an overview,” Biointerface Research in Applied Chemistry, vol. 11, no. 1, pp. 7860–7870, 2021.
15. Z.-Q. Lu, F.-Y. Zhang, H.-L. Fu, H. Ding, and L.-Q. Chen, “Rotational nonlinear double-beam energy harvesting,” Smart Materials and Structures, vol. 31, no. 2, Article ID 025020, 2021.
16. M. Safaei, M. Taran, L. Jamshidy et al., “Optimum synthesis of polyhydroxybutyrate-Co3O4

Journal of Chemical Health Risks

www.jchr.org

JCHR (2024) 14(2), 2718-2724 | ISSN:2251-6727

bionanocomposite with the highest antibacterial activity against multidrug resistant bacteria," International Journal of Biological Macromolecules, vol. 158, pp. 477–485, 2020.

17. Y. Huang, C. An, Q. Zhang et al., "Cost-effective mechanochemical synthesis of highly dispersed supported transition metal catalysts for hydrogen storage," Nano Energy, vol. 80, Article ID 105535, 2021.
18. K. Kalishwaralal, S. Jeyabharathi, K. Sundar, and A. Muthukumaran, "A novel one-pot green synthesis of selenium nanoparticles and evaluation of its toxicity in zebrafish embryos," Artificial Cells, Nanomedicine, and Biotechnology, vol. 44, no. 2, pp. 471–477, 2016.
19. Y. Cao, H. A. Dhahad, M. A. El-Shorbagy et al., "Green synthesis of bimetallic ZnO-CuO nanoparticles and their cytotoxicity properties," Scientific Reports, vol. 11, no. 1, Article ID 23479, 2021.
20. Z.-f. Yu, S. Song, X.-l. Xu, Q. Ma, and Y. Lu, "Sources, migration, accumulation and influence of microplastics in terrestrial plant communities," Environmental and Experimental Botany, vol. 192, Article ID 104635, 2021.
21. H. Lu, T. Wei, H. Lou, X. Shu, and Q. Chen, "A critical review on communication mechanism within plant-endophytic fungi interactions to cope with biotic and abiotic stresses," Journal of Fungi, vol. 7, no. 9, p. 719, 2021.
22. X. Zong, X. Xiao, B. Shen et al., "The N 6-methyladenosine RNA-binding protein YTHDF1 modulates the translation of TRAF6 to mediate the intestinal immune response," Nucleic Acids Research, vol. 49, no. 10, pp. 5537–5552, 2021.
23. M. Shah, D. Fawcett, S. Sharma, S. Tripathy, and G. Poinern, "Green synthesis of metallic nanoparticles via biological entities," Materials, vol. 8, no. 11, pp. 7278–7308, 2015.
24. B. Hosnedlova, M. Kepinska, S. Skalickova et al., "Nano-selenium and its nanomedicine applications: a critical review," International Journal of Nanomedicine, vol. 13, pp. 2107–2128, 2018.A. Khurana, S. Tekula, M. A. Saifi, P. Venkatesh, and C. Godugu, "Therapeutic applications of selenium nanoparticles," Biomedicine & Pharmacotherapy, vol. 111, pp. 802–812, 2019.
25. H. Moradpoor, M. Safaei, A. Golshah et al., "Green synthesis and antifungal effect of titanium dioxide nanoparticles on oral Candida albicans pathogen," Inorganic Chemistry Communications, vol. 130, Article ID 108748, 2021.
26. O. P. Singh, G. Kumar, and M. Kumar, "Role of Taguchi and grey relational method in optimization of machining parameters of different materials: a review," Acta Electronica Malaysia, vol. 3, no. 1, pp. 19–22, 2019.